Journal of Drug Delivery Science and Technology 79 (2023) 104062

Contents lists available at ScienceDirect

Journal of Drug Delivery Science and Technology

journal homepage: www.elsevier.com/locate/jddst

Polysorbate enhanced progesterone loaded drug diffusion from macromolecular fibrous patches for applications in obstetrics and gynaecology

Omar Shafi [a], Mohan Edirisinghe [a], Francis Brako [b,*]

[a] Torrington Place, Department of Mechanical Engineering, University College London (UCL), WC1E 6BT, UK
[b] Medway School of Pharmacy, University of Kent, ME4 4TB, UK

ARTICLE INFO

Keywords:
Obstetrics
Gynaecology
Progesterone
Polyvinylpyrrolidone (PVP)
Polysorbate
Patches

ABSTRACT

Progesterone, a steroidal hormone, is used as pharmacotherapy in the clinical practice of obstetrics and gynaecology. There are however considerable bioavailability issues with the currently available formulation. Widening the range of progesterone formulations will increase the usefulness of this drug in a variety of clinical interventions. We undertook this study to create an ideal transdermal progesterone patch, which requires a reliable system to host and release drugs sustainably. This study investigates the use of a combined fatty acid, polysorbate 80 in distilled water or ethanol, with the well-known polymer polyvinylpyrrolidone (PVP). The rheology of the polymer solutions was investigated with incremental changes in either PVP or polysorbate. For each polymer solution, electrospinning was used to create fibre systems, which were characterised by scanning electron microscopy. The optimal polymer solution consisted of 2 g of PVP in 20 ml of ethanol with 4 ml of polysorbate. Performance analysis was completed by carrying out two drug release studies: direct submersion of fibres in PBS and transdermal drug delivery of fibres across a cellulose acetate membrane using Franz Diffusion Cells. The results have shown that the polysorbate loaded fibre systems reached near 100% drug release (over two weeks) and nearly 5 times faster than the fibres without polysorbate. This confirms the penetrative enhancing capabilities of polysorbate widely presented in literature. Kinetic release studies and geometric models were also used to observe the experimental behaviour compared to expectations. Experimental results closely fit both the Makoid Banakar model and the Geometric Equation.

1. Introduction

Progesterone, a steroidal hormone produced by the ovaries has a wide range of pharmacotherapeutic uses in obstetrics and gynaecology. These range across fertility treatments, prophylactic interventions in pregnancy to palliative treatment in patients suffering from advanced or recurrent endometrial cancer. Considering prevalent challenges associated with conventional delivery of progesterone, a transdermal delivery system with controlled-release functionality will help widen the options and possibilities of accessing the immense benefits offered by this exogenous hormonal drug [1].

Progesterone is key for pregnancy maintenance and works by initially sustaining a healthy uterine lining, followed by maintaining the uterus in a quiescent state [2]. On average, 15 million infants are born premature every year, leading to early years' developmental issues and detrimental effects such as retinopathy and death [3,4]. It is also important to consider the lack of advanced neonatal intensive care units due to lack of equipment and skilled workforce in the low – middle income countries, whereby the lack of adequate (or appropriate or optimal) drug delivery access may add to the stresses of the medical issue [5]. Progesterone has been shown to reduce preterm birth before 37 weeks by 48% compared to control (OR 0.52, 95% CI 0.36–0.73); across 15 studies) and before 34 weeks, by 55% (OR 0.45, 95% CI 0.23–0.81; across 9 studies) [6], OR and CI indicate odds ratio and confidence intervals, respectively.

The therapeutic effects have been shown across a number of gynaecological conditions. Management of abnormal uterine bleeding (AUB), a common gynaecological condition which accounts for nearly 70% of clinical attendances in (peri)menopausal women, requires progestins to decrease symptoms of dysmenorrhea (painful periods) and

* Corresponding author.
E-mail address: f.brako@kent.ac.uk (F. Brako).

https://doi.org/10.1016/j.jddst.2022.104062
Received 18 July 2022; Received in revised form 24 November 2022; Accepted 3 December 2022
Available online 14 December 2022

metropathia haemorrhagica (irregular, heavy bleeding associated with cystic hyperplasia in the endometrium) [7]. It is a common successful treatment for women suffering from heavy menstrual bleeding, and is also used when treating peri-pubertal menstrual disorders [8]. Progesterone treatment can improve menstrual regulation and postpone periods, supporting those with deficient luteal phase. In other conditions, such as polycystic ovarian syndrome (PCOS), premenstrual syndrome (PMS) and fibroids, patients can be given progesterone to essentially stop periods: immediately alleviating symptoms. Progesterone is the main modality of treatment in long term endometriosis management, where endometrial cells (the monthly bleeding cells) are found outside of the uterus in the peritoneal cavity or for extra pelvic endometriosis cases such as thoracic endometriosis [9]. It is not always possible to surgically excise all rogue cells, thus the drug is used to inhibit growth of these extra-uterine endometrial cells, lessening or restricting menstruation and alleviating symptoms altogether.

There has been an increase in endometrial hyperplasia cases in young women, which can lead to endometrial cancer and can be attributed to factors such as obesity (predicted to increase by approximately 8% in the UK) [10]. Atypical hyperplasia is the least common type, but is most likely to co-exist with or a 30–50% chance to progress to endometrial carcinoma, whereas simple hyperplasia has a lower risk of progression to malignancy and both can be treated with progestin therapy [11]. High doses of progesterone are used to alleviate symptoms for patients with endometrial cancer, allowing them to bypass the need for hysterectomy, allowing for childbearing, or if surgical treatment cannot be offered due to risk for medical comorbidities. Currently, oestrogen is used for hormone replacement therapy to alleviate symptoms such as hot flushes. However, if the patient still has a uterus, then progesterone must be used to prevent endometrial hyperplasia. In cases of secondary amenorrhea, whereby regular or irregular periods are followed by long term absence of menstruation, progesterone is prescribed for a few days to induce bleeding to prevent hyperplasia and restore menses.

With growing interests in this hormone, it is key to investigate and improve the delivery of progesterone to maximise its health benefits. In current clinical practice, progesterone is available in the following oral and vaginal forms; Cyclogest® pessaries (200, 400 mg), Utrogestan® capsules (oral and vaginal) (100, 200 mg) and Crinone® gel (90mg/dose) [12]. It is also available as an injectable, Depo Provera (150 mg/ml) and Lubion® (25 mg) [13,14]. Progesterone can also be delivered from an intrauterine device, such as the Mirena coil (releasing 20 μg daily), or as an implant (Nexplanon starting at 45 μg to 25 μg by the end of the 3 year period).

The commonly used oral and vaginal route for delivery has challenges: for oral medication, a majority of the API (progesterone) is lost to hepatic metabolism [15]. Other restrictions include discomfort or the insertion of drug into the vagina may not be culturally acceptable to groups of women from certain countries [16]. A more acceptable, accessible and easier method of delivering medication is via the patch, which has seen success in delivering API's such as nicotine. However, there lacks a progesterone only patch and the closest option is the contraceptive patch, EVRA, releasing both oestrogen (33.9 μg) and progesterone (203 μg) daily [17]. The benefits of using transdermal patches are ample underscoring the high interest of introducing nanotechnological methods of fabrication.

Electrospinning (ES) is the processing method used to create progesterone loaded fibres in this study. The method has found success in fibre and scaffold fabrication for chemical, electrical and medical applications. ES requires a polymer solution to be injected through a needle (the positive electrode) that is connected to the high voltage ramp. The polymer solution is spun onto a collector plate (the negative electrode). The polymer solution is fed through the needle at constant rate. Due to the potential difference between both electrodes, the polymer solution is drawn many times before reaching the collector plate. When the solution leaves the needle (as a jet of charged particles), a Taylor cone is produced due to the electrostatic repulsion overcoming the surface tension of the fluid and reaching a prerequisite level determined by the solution in question. The droplet that emerges from the needle is altered from a circular shape to the conical, Taylor cone. As the electric field is increases, the polymeric jet stream traverses through a stable zone, and once it surpasses this, it experiences whipping and bending instabilities [18]. The jet draws many times until it begins collecting on the plate, travelling through air (evaporating the solvent) and leaving behind fibres. Solvent properties, polymer viscosity and external factors such as temperature and relative humidity all play a part in addressing the final fibre features.

Biocompatible, non-toxic, water soluble polyvinylpyrrolidone (PVP), has been used in a variety of fibre applications as it is able to encapsulate both hydrophilic and lipophilic drugs [19]. When combined with other polymers or drugs, poorly soluble drugs are infused into its structure, increasing bioavailability, highlighting opportunity for controlled release. For these reasons, PVP has been used as the skeleton for future transdermal patch creation [19]. A non-ionic surfactant, polysorbate 80, has been used to investigate its penetration abilities for drug delivery [20]. The emulsifier, having a composition including oleic and palmitic acid, is currently widely used in the cosmetic and skin industry. Surfactants alone, are known to increase the net charge density when electrospinning fibres alongside the instability of charged jet motions. This in turn, stretches the fibre's more finely, thus reducing beads in structures and increases homogeneity. This not only leads to higher surface to volume ratio (of fibre surface area to the volume it occupies) but allows for consistency if intending to infuse medication.

Previous work has successfully introduced progesterone into nanofibres [21,22]. However, no study has reported the manufacture and performance of systems for transdermal drug release specifically in comparison with surfactant. That is the core premise behind this study. In this work, 3 characterisations were conducted. Firstly, the rheology of different compositions of polymer solutions (constituting of various surfactant and polymer concentrations) were analysed followed by electrospinning of each respective solution. Scanning electron microscopy was used to determine the morphology and diameter differences. Once the optimal polymer solution and respective fibre diameter was found, progesterone was incorporated into the solution in preparation for drug release studies. The solution that was able to incorporate progesterone and surfactant, and had the lowest viscosity and cross sectional diameter was chosen as this increases both surface to volume ratio and transdermal penetration [23]. The study releases drugs into the non-toxic phosphate buffer saline (PBS), commonly used in research as it maintains a pH level of 7.4 simulating human bodily fluids. The ion concentration and osmolarity also closely match blood serum, making it an ideal product to use for such studies. Two methods of drug release were studied. Firstly, directly submerged fibre drug release; to investigate the effects of drug release in PBS. Secondly, transdermal drug release across a cellulose acetate membrane also in PBS. Both experiments will elucidate the effects of polysorbate 80 on drug release.

2. Experimental DETAILS

2.1. Materials

PVP (Luvitec K90 powder, Mw ~ 1,000,000 $gmol^{-1}$), Polysorbate 80 (Mw ~ 1310 $gmol^{-1}$), progesterone (Mw~ 314 $gmol^{-1}$) and ethanol were obtained from Sigma Aldrich, Dorset, UK. All were used without further purification. Cellulose acetate membranes of 0.22 μm pore size were used for permeation studies; these were obtained from Sartorius, Gottingen, Germany. Phosphate Buffer Saline tablets from Sigma Aldrich, Dorset, UK, were used to prepare simulation fluid of pH = 7.4.

Table 1
Ratios of PVP and polysorbate in solvent.

Tests	Polymer Solution (% (w/v) PVP in 20 ml solvent)	Addition of Polysorbate 80 (ml)	Total % (Ratio between polysorbate volume and polymer solution volume $V_{polysorbate}/V_{polymer\ solution}$)	Total % (Ratio between polymer weight and polysorbate volume $W_{PVP}/V_{polysorbate\ 80}$)
A	13%	0	0	
		3	15%	
		4	20%	
		5	25%	
		6	30%	
B	9%	4		45%
	10%			50%
	12%			60%
	13%			65%
	14%			70%

2.2. Methods

2.2.1. Preparation and characterisation of polymer solutions

Uniform mixtures of PVP blends with Polysorbate, shown in Table 1 were obtained by continuously stirring for 10 min. The Brookfield Viscometer DV-III+ (Brookfield, Middleboro, MA, USA) was used to measure the viscosities of the solutions at varying shear rates and stresses, in ratios shown in Table 1.

2.2.2. Rheology

The power law, $\sigma = K\dot{\gamma}^n$ was used to define rheology; taken from the Herschel- Bulkley equation [24], where σ is the shear stress in the fluid, K is constant and $\dot{\gamma}$ is the shear rate (s^{-1}) and n is the flow index of the solution. For $n = 1$, the mixture is Newtonian, n < 1, the fluid is pseudoplastic and when n > 1, the fluid is dilant [24].

2.2.3. Fibre preparation and characterisation

Each solution shown in Table 1 was electrospun in attempting to produce fibres. Not all solutions created fibres. The polymer viscosity was compared to the fibre diameter and then the thinnest fibre diameters (with polymer solvent that dissolves progesterone) was chosen to incorporate progesterone (at $40mg_{progesterone}/ml_{ethanol}$). The electrospinning needle, with 0.838 mm inner diameter and 1.270 mm outer diameter, was subject to a voltage of ~20 kV for the water-based solution and 8 kV for the ethanol-based solution, the relative humidity was ~45%, the temperature was ~23 °C and the needle height to plate was 150 mm. The polymer solution was fed at a consistent rate of 30 μl min^{-1}. The solution flowed for approximately 10 min. The fibres were collected on carbon taped SEM studs to prepare for imaging. The surface of the samples were gold sputter coated for 90s using (Q150R ES, Quorum Technologies). Scanning electron microscopy (Hitachi S-3400n) was used to then image the gold sputtered fibres at an accelerating voltage of 5 kV. ImageJ was used to measure the diameters of the fibres, data was extracted to Microsoft Excel for data analysis by Python and OriginPro was used to produce the fibre diameter distribution plot. A comparative analysis between progesterone loaded fibres, with and without polysorbate, named 'wet' and 'dry' respectively was conducted. The experimental control was the dry fibres. The surface tension for the solutions were characterised using a calibrated Kruss tensionmeter (Kruss GmbH, Hamburg, Germany).

2.2.4. Drug loading

The progesterone content within the fabricated fibres was determined by the standard UV assay at a wavelength of 270 nm [25]. 20 mg of fibre was dissolved in 20 ml of absolute ethanol in a volumetric flask. The flask was swirled for 24 h to ensure complete dissociation between progesterone and polymer fibres, in ethanol. 3 ml of solution was then sifted through a filter, drawn into a cuvette and analysed spectrophotometrically at 270 nm using a Jenway 6305 UV/Visible spectrophotometer (Bibby Scientific, Staffordshire, UK). The percentage loading was calculated by the drug content in a given weight of fibre as a percentage and the encapsulation efficiency was calculated by evaluating the ratio between experimental drug found in 20 mg of fibres and the theoretical drug expected in 20 mg of fibres. The calibration curve in Fig. 1, was created in preparation for the cumulative drug release studies.

2.2.5. Release studies

Two categories of *in vitro* drug release studies were undertaken: PBS for direct submersion and PBS for Franz Diffusion Cell testing with cellulose acetate membranes of pore size 0.2 μm. Cellulose acetate was used for its high correlation with natural membranes [26].

2.2.5.1. Direct submersion. 20 mg of fibres were directly submerged into PBS. The fibres were placed into a PBS bath under a constant

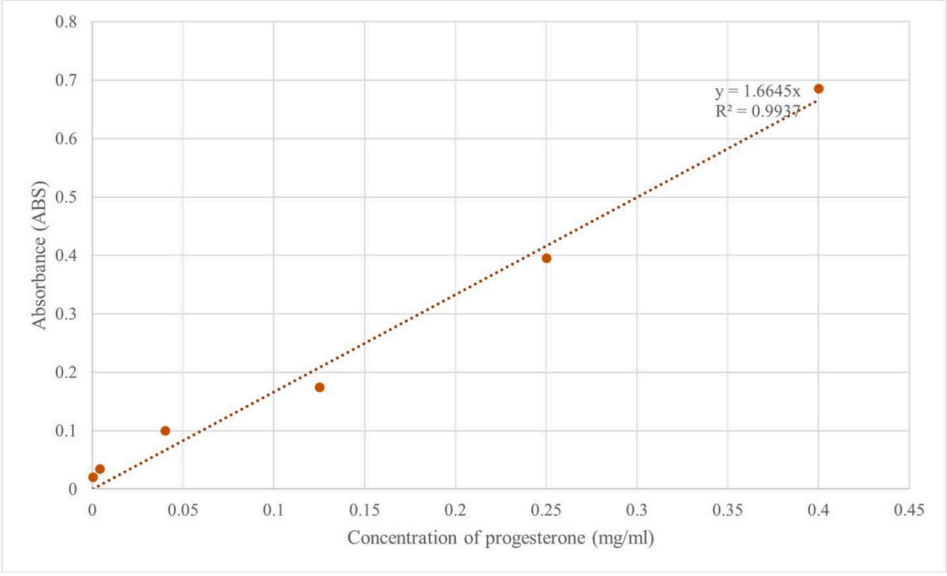

Fig. 1. Calibration curve for progesterone dissolved in ethanol.

Table 2
Models and details used to estimate drug delivery. k_0, k_1, k_H, k_{HC}, k_{MB} and k_{HB} are the release rate constants for each respective model, t is time and F is percentage released. DDsolver programming was used [27].

Model	Equation
Zero Order Model	$F = k_0 t$
First Order Model	$F = 100[1 - e^{(-k_1 t)}]$
Higuchi Model	$F = F_0 + k_H t^{0.5}$
Hixson Crowell Model	$F = 100[1 - (1 - k_{HC} t)^3]$
Makoid- Banakar Model	$F = k_{MB} t^n e^{-kt}$
Hopfenberg Model	$F = 100[1 - (1 - k_{HB} t)^n]$

Table 3
Surface Tension changes with Polysorbate addition.

	Solvent	
Polysorbate	Water (mN/m)	Ethanol (mN/m)
No	31.5 ± 3.8	21.7 ± 2.0
Yes	27.1 ± 5.3	14.1 ± 2.9

temperature of 37°C to simulate body temperature, with a magnetic stirrer in the bath for constant mixing. At predetermined timepoints, 3 ml of solution was sampled and immediately replaced with 3 ml fresh PBS solution. The amount of progesterone released was determined using UV Spectrophotometry.

2.2.5.2. Transdermal. 20 mg of fibres were placed on the surface of the artificial membrane. The membrane was placed into the Franz Diffusion Cell and the surrounding exposed areas were sealed. The top of the Franz diffusion cell orifice of 25.4 mm outer diameter was covered with parafilm, and pierced, to increase pressure in the fibre system. The Franz Diffusion Cell (volume of 3 ml) was kept under a constant temperature of 37°C to simulate body temperature, with a magnetic stirrer in the bath for adequate mixing of progesterone transported through one membrane into the buffer solution of the accepting changer. 1 ml of solution was taken in intervals and concentrations were recorded. Once 1 ml was extracted, immediately, 1 ml of PBS was replaced into solution.

2.2.6. Drug dissolution quantitative modelling

Six different models described in Table 2 were used to study progesterone release.

2.2.7. Drug diffusion geometric modelling

Geometric modelling was used to compare the release of drug from cylindrical fibres into PBS [28]. The major equations describing the models are given below. C indicates the average concentration inside the fibre at time (t), radius of cylindrical fibre (a), radial distance of drug release (r), release constant (n) and diffusion coefficient (D).

$$\frac{\partial C(r,t)}{\partial t} = D\left(\frac{\partial^2 C(r,t)}{\partial r^2} + \frac{2}{r}\frac{\partial C(r,t)}{\partial r}\right) \quad (1)$$

$C(r,0) = C_0$ for $r \leq a$

$C(a,t) = 0$ for $r > a$ for all t

For the average concentration (C_{av}) inside the fibres at time *t*,

$$C_{av}(t) = \frac{6C_0}{\pi^2}\sum_{n=1}^{\infty}\frac{1}{n^2} exp\left(\frac{-Dn^2\pi^2 t}{a^2}\right) \quad (2)$$

$$= C_0\left[1 - \frac{6(Dt)^{1/2}}{a\pi^2} - \frac{3Dt}{a^2}\right] + \frac{12(Dt)^{1/2}}{a}\sum_{n=1}^{\infty} ierfc\left(\frac{na}{(Dt)^{1/2}}\right) \quad (3)$$

Where *ierfc* is the integral of the complementary error function. The diffusion coefficient D is adjusted in results for optimal curve fitting. $C_{av}(t)/C_0 = 1\text{-}Q(t)/Q_0$, Q denotes the amount of drug, where Q(t) is the amount of Q_0 that has been released from the fibre. We made three observations: the fractional release depends on one parameter, $(Dt)^{1/2}/a$; the fractional release saturates for long times at a value of 1; the short-time release has the form $Q(t)/Q_0 \approx 6(Dt)^{1/2}/(\pi^{1/2}a)$. Therefore, we find the solutions:

$$Q_a\left(t\right) = \tanh\left(\frac{6(Dt)^{1/2}}{\pi^{1/2}a)}\right) \quad (4)$$

Which fits the expressions from equations (2) and (3).
Another fit can be obtained by using:

$$Q_b\left(t\right) = \tanh\left(\frac{\beta(Dt)^{1/2}}{a}\right) \quad (5)$$

where $\beta = 3.345$.

2.2.8. Statistical analysis

T-tailed t tests were conducted to compare the comparative significance between wet and dry fibres, for diameter differences and drug release differences. P significances are found in the respective figures. The average of the Root Mean Square Error (RMSE) across wet and dry fibres was used to compare the average difference between predicted and observed drug release data.

3. Results and discussion

3.1. Rheology

3.1.1. Effect of varying concentrations of either polysorbate or PVP

The corresponding shear stress and viscosity graphs are given in supplementary information, Figs. S1 and S2 respectively. For all cases in Fig. S1, the trend of shear stress increasing with shear rate suffices the power law. When calculating the flow index of solutions using the power law ethanol-based solutions all resulted in $n \simeq 1$ suggesting that the solutions were near Newtonian. However, as a result of the immiscibility of polysorbate in water-based solutions, there was a fluctuation as a few polymeric solutions resulting in $n \leq 1$, suggesting that the solutions were either Newtonian or Pseudoplastic, see Table S2.

In ethanol, as polysorbate increased, there was an adverse effect compared to when using water and the viscosity reduced, see Figures S2a and S2 b. Micelles were not formed and surface tension was reduced (from 31.5 mN/m to 21.7 mN/m, as shown in Table 3); this is due to the alkyl chain in the polysorbate being soluble in alcohol. The increase in critical micelle concentration (CMC) suggests that (hydrophilic) ethanol caused a lower average viscosity compared to that of water, and also satisfies the inverse relationship in the surface tension equation [29]. From visual analysis, it was clear that ethanol and polysorbate were miscible compared to when mixed with water, in the latter the polysorbate just sat on top of the PVP solution a few minutes after speed mixing.

When adding PVP, viscosity incrementally increased in both water and ethanol-based solutions (Figure S2c and S2 d). The increase is expected due to the behaviour of PVP [30] and may be due to the reduction in surface porosity as the molecular weight of PVP K90 is high; shown to influence the phase separation kinetics and thus increasing viscosity [31]. The average viscosities were smaller in the ethanol solutions than in water.

In water the viscosity increased with polysorbate concentration, albeit the largest increase in viscosity was observed between 5 ml and 6 ml. This is due to the CMC being surpassed, at which point, viscosity increases far more rapidly as the surface became saturated [32,33]. When surfactants are introduced into polymer solutions, the interactions between the constituents generates surfactant-polymer aggregates [34]. This rise can be explained by the 'necklace model', whereby the polymer

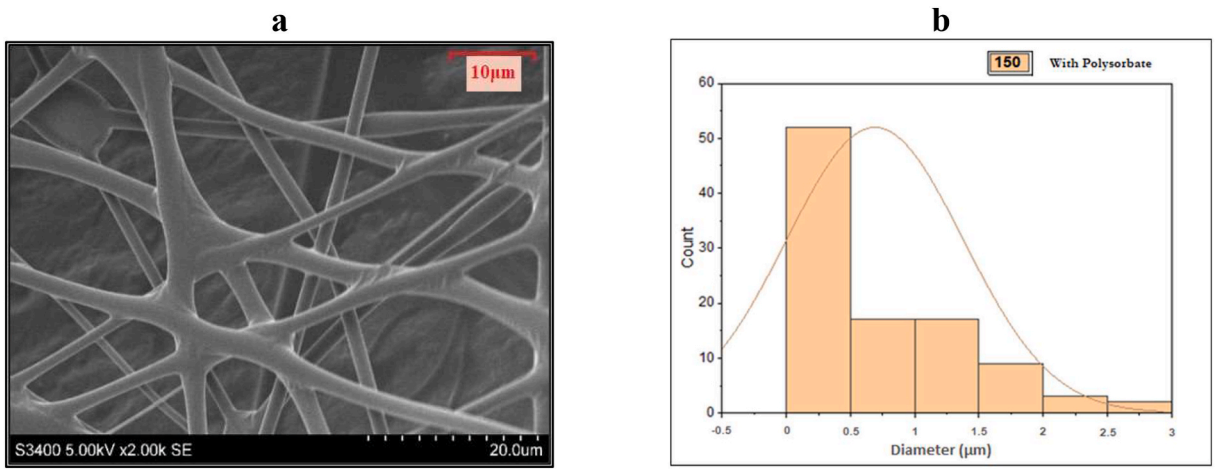

Fig. 2. SEM results of microfibers and the related fibre diameter distribution.

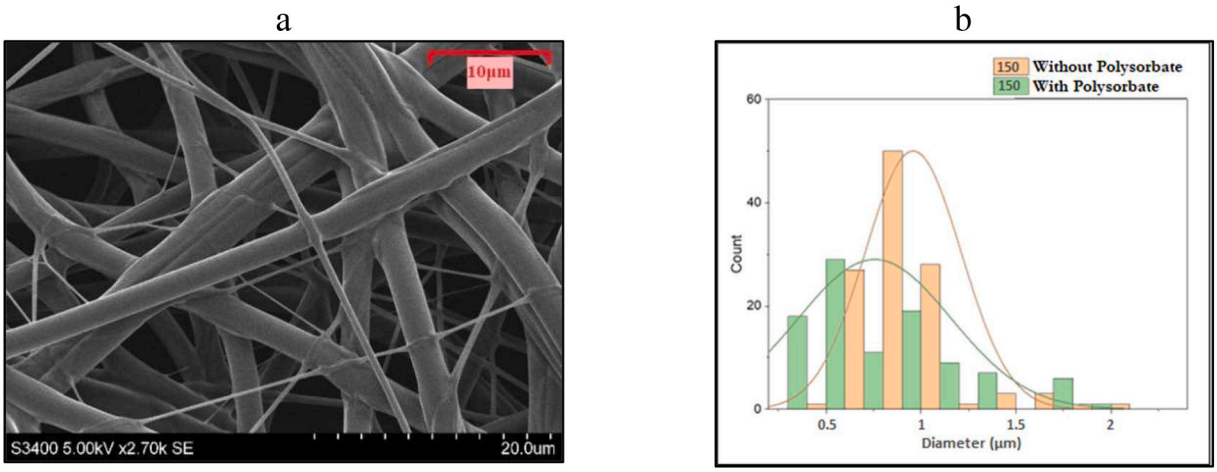

Fig. 3. Progesterone loaded fibres (a); diameter distribution comparing both ($p < 0.05$) (b).

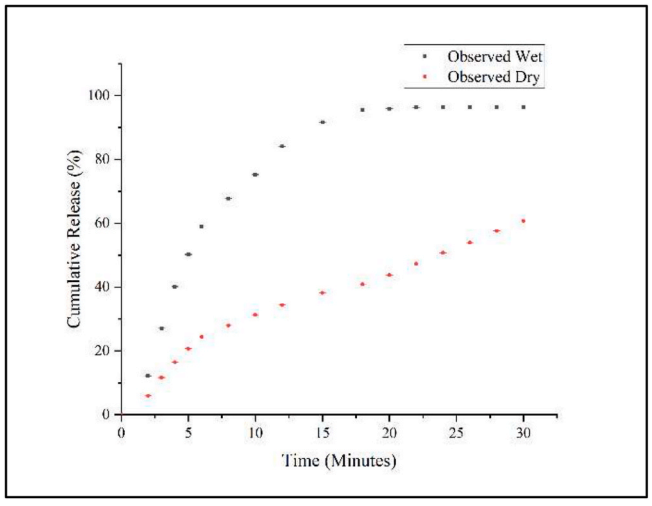

Fig. 4. Direct submersion: Progesterone drug release in PBS ($p < 0.05$).

macromolecule encloses the surfactant micelles, and then its segments permeate into the polar head group of the micelles, protecting their hydrophobic tails from water [35]. These interactions, occurring at favourable sites, of coiled polymer macromolecules can lead to shrinking, extensions and the bridging of polymer macromolecules; consequently, having effects on the rheological behaviour and homogeneity of solutions [34]. Wang et al. [32] have shown that the non-ionic surfactant (polysorbate) used, compared to anionic and cationic surfactants, had a larger increase in viscosity. This surfactant creates prolate ellipsoid micelles which provides physical cross linking creating a resistance to deformation when subject to external shear stress, which in turn increases viscosity [36]; polysorbate has been shown to have this structure [37]. The viscosity that reduced as polysorbate increased in the ethanol solution can be explained by alcohol reducing the interfacial tension in the solution [38].

Data in Fig. S2 shows that at higher shear rates, the viscosity is near stability. At lower shear rates, there is greater fluctuation. This is due to the molecules having favoured conformations which may not be oriented well in the direction of flow, causing resistance hence leading to a relatively higher viscosity. However, at higher shear rates, the molecules align with the spindle, reducing resistance and providing a lower viscosity. The decrease in the viscosity as shear rate increases is known due to the entangled chain networks in the polymer solution, and with higher viscosities a more homogenous spread of solvent molecules over the entangled polymer occurs [39].

3.2. Rheology and morphology optimisation

3.2.1. Surface tension and chosen solvent

When deciding the final solvent for the polymer solution to be spun,

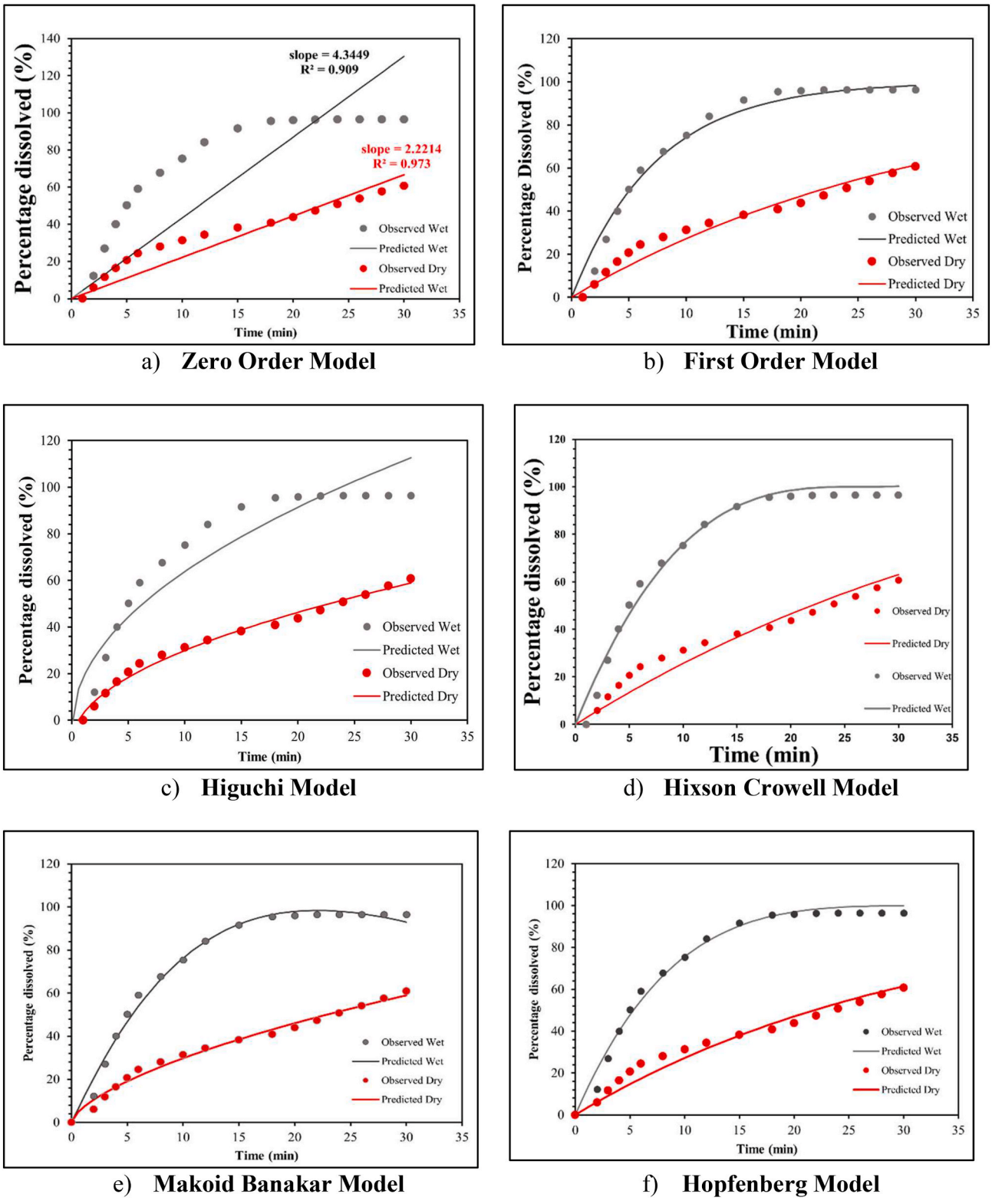

Fig. 5. Kinetic Release Models for fibres submerged directly in PBS.

ethanol was chosen over water. Firstly, micelles formed with water and did not achieve complete homogeneity in the polymer solution (the water solution was required to be constantly speed mixed prior to spinning and increased processing time). Secondly, because progesterone dissolved in ethanol.

The chosen polymeric solutions for both ethanol and water underwent surface tension studies. It is clear from the results that ethanol-based solutions had lower surface tensions. The polysorbate also had an effect on reducing surface tension in both solutions. This reflected the results of the viscosities, and therefore, the resulting diameters of electrospun fibres.

Table 4
Average RMSE values between Predicted and Observed Data.

Model	Average RMSE
Zero Order Model	**31.1**
First Order Model	14.8
Higuchi Model	20.9
Hixson Crowell Model	16.0
Makoid Banakar Model	**11.5**
Hopfenberg Model	14.0

Table 5
Constants for wet and dry fibres.

Model	Parameters for Wet Fibres	Parameters for Dry Fibres
Zero Order Model	$k_{o\ -wet} = 4.3$, $RMSE = 46.4$	$k_{o\ -dry} = 2.2$, $RMSE$
First Order Model	$k_{1\text{-}wet} = 0.14$	$k_{1\text{-}dry} = 0.03$.
Higuchi Model	$F_{0\text{-}wet} = -2.9$, $k_{H\text{-}wet} = 21.1$,	$F_{0\text{-}dry} = -9.6$, $k_{H\text{-}dry} = 12.5$
Hixson Crowell Model	$k_{HC\text{-}wet} = 0.04$.	$k_{HC\text{-}dry} = 0.009$.
Makoid Banakar Model	k_{MB}.wet = 10.9, n-wet = 1.1, k-wet = 0.05.	k_{MB} dry = 6.7, n-dry = 0.7, k-dry = 0.002.
Hopfenberg Model	K_{HB}-wet = 0.03, n-wet = 4.4.	K_{HB}-dry = 0, n-dry = 2722.4

Table 6
Average RMSE values between Predicted and Observed Data.

Model	Average RMSE
Geometric Model Equation 4	**23.0**
Geometric Model Equation 5	23.5

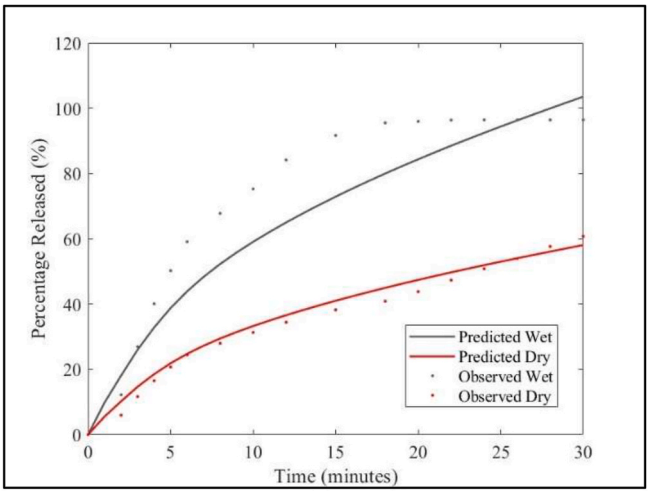

Fig. 6. Geometric Model for Drug Release of Submerged Fibres.
$D_{dry} = 1.8 \times 10^{-17}$, $R_{dry} = 479$ nm, $Dry_{max} = 0.28$. $D_{wet} = 4.1 \times 10^{-16}$, $R_{wet} = 395$ nm, $Wet_{max} = 0.09$.

3.2.2. Fibre morphology

3.2.2.1. Fibre diameters vs concentration of PVP in solvent. Fig. S3 shows the different diameters that have been generated at respective solutions. Fibres were not generated for all solutions. If the viscosity was too small, fibres would not form and the solution would spray across the grounding electrode and if too large the needle would get clogged. Two interesting observations were made. Although the ethanol solutions have lower viscosities than the water based solutions, the fibres were of higher diameter; this has been observed in other water based polymer experiments, suggesting the faster evaporation of solvent may play a part in determining diameter [40,41]. When increasing the polysorbate concentration, the average diameter increased. Increase in diameter was also observed as PVP concentration increased when polysorbate remained constant. In order to streamline towards an optimal structure, the lowest viscosity fibre producing solution with polysorbate and a progesterone dissolving solvent were chosen, due to maximum surface area to volume ratio as well as drug loading discussed below.

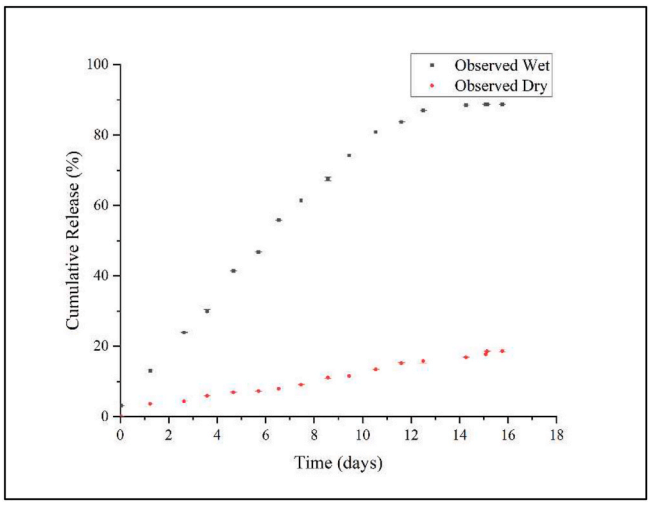

Fig. 7. Transdermal drug release of progesterone ($p < 0.05$).

3.2.3. Chosen polymer solution: 2 g of PVP in 20 ml (Ethanol) + 4 ml (Polysorbate)

With the use of ethanol contributing to the complete mixing of polymer solution and surfactant, the SEM analysis successfully showed the average fibre diameter distribution to be 690 nm (Fig. 2). This polymer solution consisted of the highest amount of polysorbate without compromising the surface area to volume ratio. Smooth fibres were formed with no observed beads, thus showing promise for controlled drug release. Amongst all other polymer solutions, this was chosen to have progesterone.

3.2.4. Introducing progesterone into chosen polymer solution

The polysorbate reduced the average fibre diameter distribution of the loaded fibres from 960 nm to 760 nm. Ethanol, compared to water, drastically reduced the surface tension (see Table 3), which in turn, reduced the potential required to overcome the electrostatic repulsion and initiate the Taylor cone, from 24 kV to 8 kV. Above the respective voltages, fibres were not formed and crystallisation occurred at the needle tip. All other conditions remained the same.

It was interesting to analyse the effects of including water as a PVP and progesterone solvent. Ethanol:Water solvent ratios were analysed to assess the morphology of fibres. When using water alone as a solvent or a partial solvent, the progesterone did not dissolve fully and precipitates were formed. Therefore, as the water concentration increased, the smoothness in the fibres reduced, beads were formed and progesterone would quickly clog the needle, increasing uncertainty in how much progesterone was actually loaded into the fibres. At times, water in the solutions did not spin fibres and rather rendered as an obstacle as the polymer solution and the polysorbate would not mix fully. This would leave just polysorbate spraying alone with no polymer, thus leaving no resultant fibres. When spinning was achieved, they would embed into one another, reducing the high surface volume to area ratio; a quality to be maximised for higher drug load. The maximum amount of ethanol: water that was able to create progesterone loaded fibres was 3:2. In 100% ethanol concentration, micelles were not formed and there was no additional requirement to keep the polymer under constant stirring. Smooth fibres were only observed with ethanol (Fig. 3) and were chosen

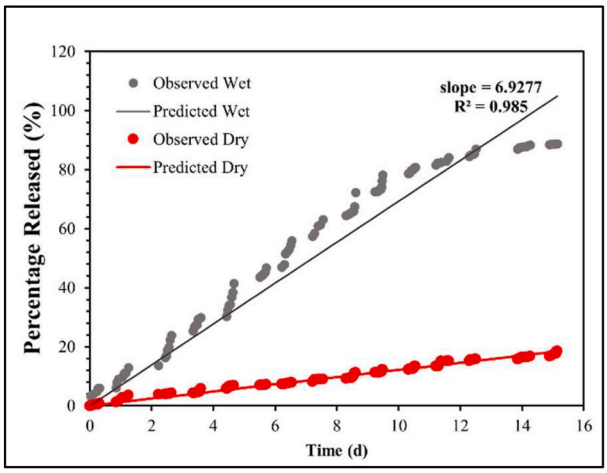

a) **Zero Order Model**

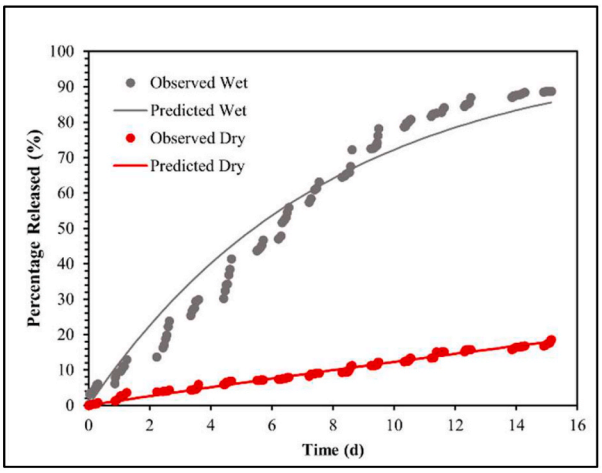

b) **First Order Model**

c)

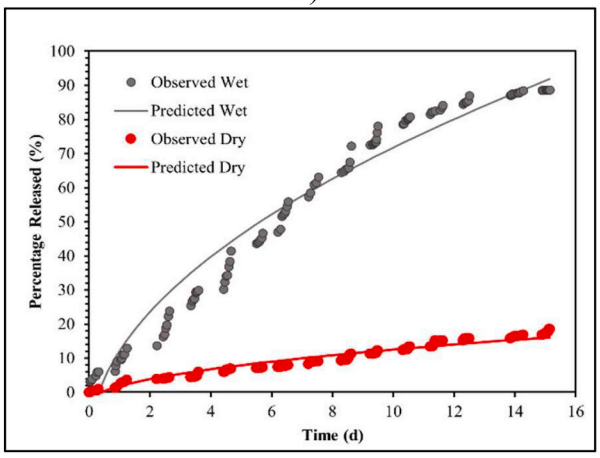

e) **Higuchi Model**

d)

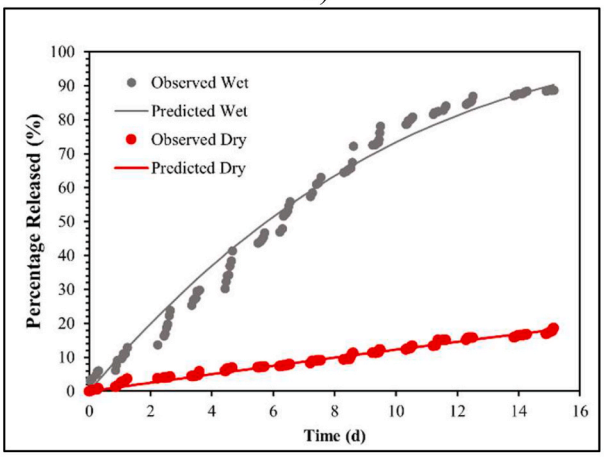

f) **Hixson Crowell Model**

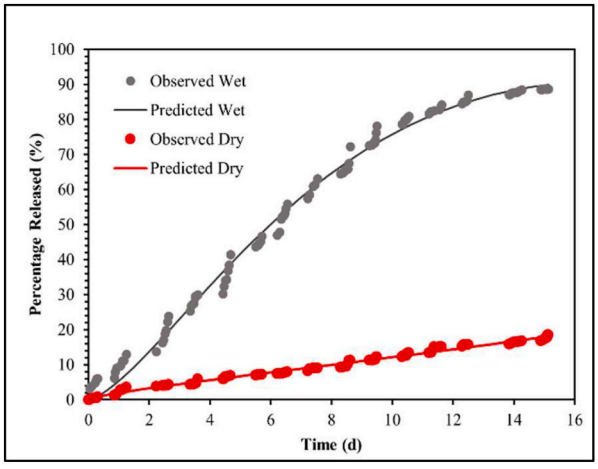

g) **Makoid Banakar Model**

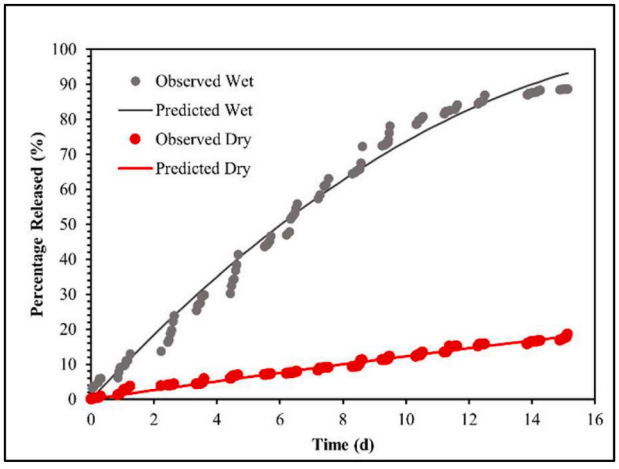

h) **Hopfenberg Model**

Fig. 8. Kinetic release modelling of transdermal drug diffusion.

Table 7
Average RMSE values between Predicted and Observed Data.

Model	Average RMSE
Zero Order Model	**13.7**
First Order Model	11.7
Higuchi Model	11.4
Hixson Crowell Model	8.8
Makoid Banakar Model	**6.9**
Hopfenberg Model	8.9

Table 8
Constants parameters for submerged fibre experiment.

Model	Parameters for Wet Fibres	Parameters for Dry Fibres
Zero Order Model	$k_{o\text{-}wet} = 6.9.$	$k_{o\text{-}dry} = 1.2.$
First Order Model	$k_{1\text{-}wet} = 0.1.$	$k_{1\text{-}dry} = 0.01.$
Higuchi Model	$F_{0\text{-}wet} = -15.3$, $k_{H\text{-}wet} = 27.5.$	$F_{0\text{-}dry} = -3.1$, $k_{H\text{-}dry} = 4.94.$
Hixson Crowell Model	$k_{HC\text{-}wet} = 0.04.$	$k_{HC\text{-}dry} = 0.004.$
Makoid Banakar Model	k_{MB}-wet = 5.8, n-wet = 1.5, k-wet = 0.1.	k_{MB} dry = 1.9, n-dry = 0.7, k-dry = −0.02.
Hopfenberg Model	K_{HB}-wet = 0.05, n-wet = 1.9.	K_{HB}-dry = 0, n-dry = 179.6.

Table 9
Average RMSE values between Predicted and Observed Data.

Model	Average RMSE
Geometric Model Equation 4	**14.8**
Geometric Model Equation 5	15

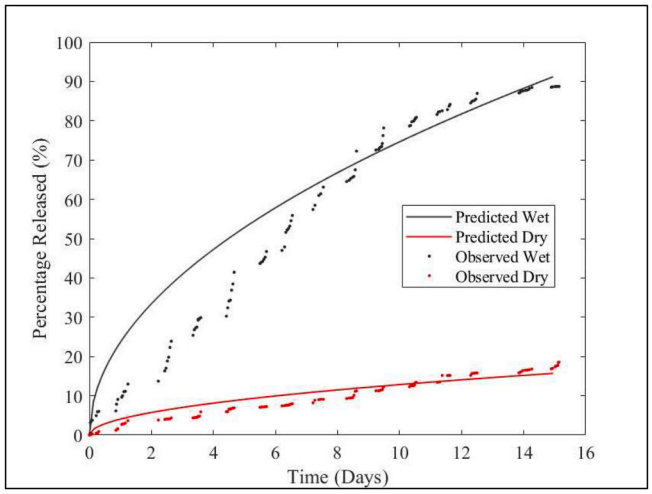

Fig. 9. Geometric Model for Transdermal Drug Release $D_{dry} = 2.6 \times 10^{-18}$, $R_{dry} = 479$ nm, $Dry_{max} = 0.28$. $D_{wet} = 6.3 \times 10^{-16}$, $R_{wet} = 395$ nm, $Wet_{max} = 0.09$.

for further drug release studies. A summary of all fibre morphology and rheology results are presented in the supplementary information (Fig. S3 and Table S1).

3.3. Encapsulation efficiency

The encapsulation efficiency for the dry fibres was 84% and for wet fibres, 73%.

3.3.1. Direct submersion release

3.3.1.1. Experimental data. Fig. 4 shows a burst release occurring for both vehicles [42]. Wet fibre progesterone release reached approximately 72% within the first 10 min and 98% within half an hour. However, the dry fibres reached 25% progesterone release within 10 min and 60% after 30 min. The faster drug release rate from the wet fibres is attributed to the surfactant characteristic of increasing dosage hydrophilicity, hence inducing drug dissolution [43]. The predicted models are superimposed upon the observed experimental data.

3.3.1.2. Kinetic Release Modelling. The model with the largest average RMSE across both wet and dry fibres was the Zero Order Model (Fig. 5a), $RMSE_{SUBMERGED} = 31.1$. The model with the smallest average RMSE across both wet and dry fibres was the Makoid Banakar Model (Fig. 5e), with the average $RMSE_{SUBMERGED} = 11.5$. See Table 4 for all RMSE results. For all cases, the release constants are considerably higher when polysorbate is infused into the progesterone loaded fibres. This is expected due to the faster overall release in the wet fibres compared to that of the dry fibres, see Table 5.

3.3.1.3. Geometric modelling. Between the two solutions from the Geometric Model, equation (4) outputted the lowest average RMSE, see Table 6. For the submerged experiment, the drug release for the observed wet fibres indicate biphasic release, burst then sustained (Fig. 6). The remaining releases for observed dry, predicted wet and dry are all indicating burst release. The diffusion coefficient, as expected, is higher in the wet fibres than that of the dry fibres. This suggests that the polysorbate played a crucial role in increasing diffusion of drug into PBS due to its penetrative enhancing characteristics.

3.3.2. Transdermal release

3.3.2.1. Experimental data. In Fig. 7, wet fibres had a much faster release reaching 89% within just over two weeks. At that same point, progesterone release from the dry fibres reached approximately 18% within the same time frame. Polysorbate is well known for its penetration enhancing capabilities by increasing drug diffusion through intercellular lipid bilayers of skin and raising the thermodynamic activity of the drug by emulsifying the sebum (oily substance excreted by sebaceous glands) [44]. This is witnessed both in this study, in PBS and through the artificial transdermal membrane. For this study, wet fibres released progesterone through a transdermal membrane nearly 5 times faster than dry fibres. This promising result through an artificial membrane provides support for polysorbate as a penetration enhancer as percutaneous drug absorption in clinical practice requires drugs to diffuse through more obstructions including hair follicles and sweat ducts [23].

3.3.2.2. Kinetic Release Modelling. The predicted models are superimposed upon the observed experimental data. The model with the largest average RMSE across both wet and dry fibres was the Zero Order Model (Fig. 8a), with the average $RMSE_{TRANSDERMAL} = 13.7$. The model with the smallest average RMSE was the Makoid Banakar model (Fig. 8e), with the average $RMSE_{TRANSDERMAL} = 6.9$. For all average RMSE results, see Table 7. Therefore, the optimal model for estimating the experimental data was the Makoid Banaker Model. For all cases, the constants are considerably higher when polysorbate is infused into the progesterone loaded fibres. This is expected due to the faster release timings in the wet fibres compared to that of the dry fibres, see Table 8.

3.3.2.3. Geometric modelling. Between the two solutions from the Geometric Model, equation (4) outputted the lowest average RMSE, see Table 9. For the transdermal experiment, the drug release for both predicted and observed fibres indicate controlled burst release. The

diffusion coefficient, as expected, is higher in the wet fibres than that of the dry fibres (Fig. 9). This suggests that the polysorbate played a crucial role in increasing diffusion of drug into PBS due to its penetrative enhancing characteristics.

4. Conclusions

The first part of the study investigated the effects of polysorbate on polymer, with changes in the solvent used. Clear differences in viscosity changes were observed as polysorbate increased when in water, than in ethanol. The hydrophobic behaviours of polysorbate in water created micelles and increased viscosity. Post rheology assessment, attempts were made to spin all solutions. A select few solutions were able to produce fibres, whereas other solutions were too viscous, too fluid or did not have enough PVP to hold a skeleton. At spinnable viscosities, morphology was analysed for each fibre and the fibre solution that was able to hold progesterone, produce the thinnest bead-less fibres containing polysorbate was used for progesterone delivery analysis. Drug release studies showed the benefits of using polysorbate in the patch. For both transdermal and direct submersion, maximum progesterone release was reached at an observably faster rate when polysorbate was introduced and proved useful for future patch exploration. Analysis of kinetic models concluded that the Makoid-Banakar model fit most closely compared to all other models.

Author contributions

All authors contributed to the writing and editing of the manuscript. **Omar Shafi** conducted the research, designed and executed the experiments followed by data analysis. **Francis Brako and Mohan Edirisinghe** collectively supervised and managed the overall aspects of the research.

Author statement

We thank you and the editor for the constructive feedback. Each issue raised has been addressed accordingly and highlighted in the manuscript for easy identification.

Declaration of competing interest

The authors declare that there is no conflict of interest in the study reported.

Data availability

Data will be made available on request.

Acknowledgements

The **Consultants of London Gynaecology** are thanked for making helpful suggestions to improve the manuscript. The Sir Richard Stapley Education Trust is thanked for supporting Omar Shafi's doctoral studies at UCL.

Appendix A. Supplementary data

Supplementary data to this article can be found online at https://doi.org/10.1016/j.jddst.2022.104062.

References

[1] O. Shafi, M. Edirisinghe, U. Edirisinghe, F. Brako, Recent developments of progesterone in nano-pharmaceutical drug delivery, in: Advances in Health and Disease 43, Nova Publishers, London, 2021.

[2] M.S. Soloff, et al., Effects of progesterone treatment on expression of genes involved in uterine quiescence, Reprod. Sci. 18 (8) (2011) 781–797, https://doi.org/10.1177/1933719111398150.

[3] WHO, Preterm Birth, 2018. https://www.who.int/news-room/fact-sheets/detail/preterm-birth. (Accessed 3 December 2020).

[4] S.J. Choi, Use of progesterone supplement therapy for prevention of preterm birth: review of literatures, Obstet. Gynecol. Sci. 60 (5) (2017) 405–420, https://doi.org/10.5468/ogs.2017.60.5.405.

[5] H.O. Amadi, et al., The impact of recycled neonatal incubators in Nigeria: a 6-year follow-up study, Int. J. Pediatr. (2010), 269293, https://doi.org/10.1155/2010/269293, 2010.

[6] NIHR, Updated Evidence on Progesterone to Prevent Preterm Birth in At-Risk Pregnancies, Feb. 2019, https://doi.org/10.3310/signal-000739.

[7] M. Jewson, P. Purohit, M.A. Lumsden, Progesterone and abnormal uterine bleeding/menstrual disorders, Best Pract. Res. Clin. Obstet. Gynaecol. 69 (Nov. 2020) 62–73, https://doi.org/10.1016/j.bpobgyn.2020.05.004.

[8] S. Elmaogullari, Z. Aycan, Abnormal uterine bleeding in adolescents: management, J Clin Res Pediatr Endrocinol 10 (3) (2018) 191–197 [Online]. Available: https://www.uptodate.com/contents/abnormal-uterine-bleeding-in-adolescents-management/print?source=see_link.

[9] Y. Li, et al., Progesterone alleviates Endometriosis via inhibition of uterine cell proliferation, inflammation and angiogenesis in an immunocompetent mouse model, PLoS One 11 (10) (2016) 1–19, https://doi.org/10.1371/journal.pone.0165347.

[10] L. Keaver, B. Xu, A. Jaccard, L. Webber, Morbid obesity in the UK: a modelling projection study to 2035, Scand. J. Publ. Health 48 (4) (2020) 422–427, https://doi.org/10.1177/1403494818794814.

[11] P. Natarajan, A. Vinturache, R. Hutson, D. Nugent, T. Broadhead, The value of MRI in management of endometrial hyperplasia with atypia, World J. Surg. Oncol. 18 (1) (2020) 1–8, https://doi.org/10.1186/s12957-020-1811-5.

[12] B.N. Forumulary, PROGESTERONE | Drug | BNF Content Published by NICE, 2020 accessed Dec. 03, 2020), https://bnf.nice.org.uk/drug/progesterone.html.

[13] Pharmasure, Package leaflet: Information for the User Lubion® 25 Mg Solution for Injection, 2018. https://www.pharmasure.co.uk/uploads/lubion-patient-information-leaflet.pdf. (Accessed 3 December 2020).

[14] M.S. Piver, J.J. Barlow, J.R. Lurain, L.E. Blumenson, Medroxyprogesterone acetate (Depo-Provera) vs. hydroxyprogesterone caproate (Delalutin) in women with metastatic endometrial adenocarcinoma, Cancer 45 (2) (Jan. 1980) 268–272, https://doi.org/10.1002/1097-0142(19800115)45:2<268::aid-cncr2820450211>3.0.co;2-8.

[15] S. Malik, K. Krishnaprasad, Natural micronized progesterone sustained release (SR) and luteal phase: role redefined, J. Clin. Diagn. Res. 10 (2) (2016), https://doi.org/10.7860/JCDR/2016/17278.7212. QE01–QE04.

[16] N. Meenakshi, Taboo in consumption: social structure, gender and sustainable menstrual products, Int. J. Consum. Stud. 44 (3) (2020) 243–257, https://doi.org/10.1111/ijcs.12562.

[17] National Health Service, Hormone Replacement Therapy, HRT) - NHS, 2019. https://www.nhs.uk/conditions/hormone-replacement-therapy-hrt/. (Accessed 1 October 2020).

[18] S. Zargham, S. Bazgir, A. Tavakoli, A.S. Rashidi, R. Damerchely, The effect of flow rate on morphology and deposition area of electrospun Nylon 6 nanofiber, Dec, J. Eng. Fiber. Fabr. 7 (4) (2012), 155892501200700, https://doi.org/10.1177/155892501200700414.

[19] M. Kurakula, G.S.N.K. Rao, Pharmaceutical assessment of polyvinylpyrrolidone (PVP): as excipient from conventional to controlled delivery systems with a spotlight on COVID-19 inhibition, J. Drug Deliv. Sci. Technol. 60 (2020), https://doi.org/10.1016/j.jddst.2020.102046. June.

[20] A.F. Belhaj, K.A. Elraies, S.M. Mahmood, N.N. Zulkifli, S. Akbari, O.S.E. Hussien, The effect of surfactant concentration, salinity, temperature, and pH on surfactant adsorption for chemical enhanced oil recovery: a review, J. Pet. Explor. Prod. Technol. 10 (1) (2020) 125–137, https://doi.org/10.1007/s13202-019-0685-y.

[21] F. Brako, B.T. Raimi-Abraham, S. Mahalingam, D.Q.M. Craig, M. Edirisinghe, The development of progesterone-loaded nanofibers using pressurized gyration: a novel approach to vaginal delivery for the prevention of pre-term birth, Int. J. Pharm. 540 (1–2) (2018) 31–39, https://doi.org/10.1016/j.ijpharm.2018.01.043.

[22] C. Karuppannan, M. Sivaraj, J.G. Kumar, R. Seerangan, S. Balasubramanian, D. R. Gopal, Fabrication of progesterone-loaded nanofibers for the drug delivery applications in bovine, Nanoscale Res. Lett. 12 (1) (2017) 4–9, https://doi.org/10.1186/s11671-016-1781-2.

[23] N. Akhtar, M.U. Rehman, H.M.S. Khan, F. Rasool, T. Saeed, G. Murtaza, Penetration enhancing effect of polysorbate 20 and 80 on the in vitro percutaneous absorption of L-ascorbic acid, Trop. J. Pharmaceut. Res. 10 (3) (2011) 281–288, https://doi.org/10.4314/tjpr.v10i3.1.

[24] M. Acosta, V.L. Wiesner, C.J. Martinez, R.W. Trice, J.P. Youngblood, Effect of polyvinylpyrrolidone additions on the rheology of aqueous, highly loaded alumina suspensions, J. Am. Ceram. Soc. 96 (5) (2013) 1372–1382, https://doi.org/10.1111/jace.12277.

[25] P. Wilson, Development and validation of a liquid chromatographic method for the simultaneous determination of estradiol, estriol, estrone, and progesterone in pharmaceutical preparations, J. AOAC Int. 92 (3) (2009) 846–854.

[26] A. Khdair, I. Hamad, M. Al-Hussaini, D. Albayati, H. Alkhatib, B. Alkhalidi, In vitro artificial membrane-natural mucosa correlation of carvedilol buccal delivery, J. Drug Deliv. Sci. Technol. 23 (6) (2013) 603–609, https://doi.org/10.1016/S1773-2247(13)50092-X.

[27] Y. Zhang, et al., DDSolver: an add-in program for modeling and comparison of drug dissolution profiles, AAPS J. 12 (3) (2010) 263–271, https://doi.org/10.1208/s12248-010-9185-1.
[28] M. Eltayeb, E. Stride, M. Edirisinghe, A. Harker, Electrosprayed nanoparticle delivery system for controlled release, Mater. Sci. Eng. C 66 (2016) 138–146, https://doi.org/10.1016/j.msec.2016.04.001.
[29] T. Sidim, G. Acar, Alcohols effect on critic micelle concentration of polysorbate 20 and cetyl trimethyl ammonium bromine mixed solutions, J. Surfactants Deterg. 16 (4) (2013) 601–607, https://doi.org/10.1007/s11743-012-1429-x.
[30] T. Sato, S. Kohnosu, Effect of polyvinylpyrrolidone on the physical properties of titanium dioxide suspensions, Colloids Surfaces A Physicochem. Eng. Asp. 88 (2–3) (1994) 197–205, https://doi.org/10.1016/0927-7757(94)02779-X.
[31] E.Y. Astakhov, I.M. Kolganov, E.R. Klinshpont, P.G. Tsarin, A.A. Kalacheva, Influence of polyvinylpyrrolidone on morphology, Hydrophilicity , and Performance of Polyethersulfone Microfiltration Membranes 52 (8) (2012) 557–564, https://doi.org/10.1134/S0965544112080026.
[32] R. Esteves, N. Onukwuba, B. Dikici, Determination of surfactant solution viscosities with a rotational viscometer determination of surfactant solution viscosities with a rotational viscometer, Beyond Undergrad. Res. J. 1 (January) (2016) 12–19.
[33] Kruss, Critical Micelle Concentration (CMC) and Surfactant Concentration, 2021. https://www.kruss-scientific.com/en/know-how/glossary/critical-micelle-concentration-cmc-and-surfactant-concentration. (Accessed 10 June 2021).
[34] J. Yang, R. Pal, Investigation of surfactant-polymer interactions using rheology and surface tension measurements, Polymers 12 (10) (2020), https://doi.org/10.3390/polym12102302, 2302.
[35] R. Magarajan, lN DILUTE AQUEOUS SOLUTIONS 76 (2) (1980).
[36] S.C. Wang, T.C. Wei, W. Bin Chen, H.K. Tsao, Effects of surfactant micelles on viscosity and conductivity of poly(ethylene glycol) solutions, J. Chem. Phys. 120 (10) (2004) 4980–4988, https://doi.org/10.1063/1.1644798.
[37] A. Amani, P. York, H. De Waard, J. Anwar, Molecular dynamics simulation of a polysorbate 80 micelle in water, Soft Matter 7 (6) (2011) 2900–2908, https://doi.org/10.1039/c0sm00965b.
[38] J.S. Zhou, M. Dupeyrat, Alcohol effect on interfacial tension in oil-water-sodium dodecyl sulphate systems, J. Colloid Interface Sci. 134 (2) (1990) 320–335, https://doi.org/10.1016/0021-9797(90)90142-B.
[39] B. Dhandayuthapani, Y. Yoshida, T. Maekawa, D.S. Kumar, Fabrication and characterization of nanofibrous scaffold developed by electrospinning, Mater. Res. 14 (3) (2011) 317–325, https://doi.org/10.1590/S1516-14392011005000064.
[40] J.E. Raber-Durlacher, et al., Swallowing dysfunction in cancer patients, Support. Care Cancer 20 (3) (2012) 433–443, https://doi.org/10.1007/s00520-011-1342-2.
[41] M.C. A. Melnick L. Sheng, 乳鼠心肌提取 HHS public access, Physiol. Behav. 176 (1) (2016) 100–106, https://doi.org/10.1021/la5023104.Effect.
[42] R. Rothe, et al., Adjuvant drug-assisted bone healing: advances and challenges in drug delivery approaches, Pharmaceutics 12 (5) (2020) 1–39, https://doi.org/10.3390/pharmaceutics12050428.
[43] Mohd Yasir, I. Som, K. Bhatia, Status of surfactants as penetration enhancers in transdermal drug delivery, J. Pharm. BioAllied Sci. 4 (1) (2012) 2, https://doi.org/10.4103/0975-7406.92724.
[44] M.A. James-Smith, B. Hellner, N. Annunziato, S. Mitragotri, Effect of surfactant mixtures on skin structure and barrier properties, Ann. Biomed. Eng. 39 (4) (2011) 1215–1223, https://doi.org/10.1007/s10439-010-0190-4.